PHYSICAL REVIEW B VOLUME 52, NUMBER 6 1 AUGUST 1995-II

Finite-size effects on the vortex-glass transition in thin $YBa_2Cu_3O_{7-\delta}$ films

P. J. M. Wöltgens* and C. Dekker†
Faculty of Physics and Astronomy, and Debye Institute, Utrecht University, P.O. Box 80.000, 3508 TA Utrecht, The Netherlands

R. H. Koch, B. W. Hussey, and A. Gupta
IBM Thomas J. Watson Research Center, P.O. Box 218, Yorktown Heights, New York 10598
(Received 24 February 1995)

Nonlinear current-voltage characteristics have been measured at high magnetic fields in $YBa_2Cu_3O_{7-\delta}$ films of a thickness t ranging from 3000 down to 16 Å. Critical-scaling analyses of the data for the thinner films ($t \leq 400$ Å) reveal deviations from the vortex-glass critical scaling appropriate for three-dimensional (3D) systems. This is argued to be a finite-size effect. At large current densities J, the vortices are probed at length scales smaller than the film thickness, i.e., 3D vortex-glass behavior is observed. At low J by contrast, the vortex excitations involve typical length scales exceeding the film thickness, resulting in 2D behavior. Further evidence for this picture is found directly from the 3D vortex-glass correlation length, which, upon approach of the glass transition temperature, appears to level off at the film thickness. The results indicate that a vortex-glass phase transition does occur at finite temperature in 3D systems, but not in 2D systems. In the latter an onset of 2D correlations occurs towards zero temperature. This is demonstrated in our thinnest film (16 Å), which, in a magnetic field, displays a 2D vortex-glass correlation length which critically diverges at zero temperature.

I. INTRODUCTION

The effective dimensionality is a quantity of prime importance for the highly anisotropic cuprate superconductors. Much attention has therefore been paid to the study of ultrathin films and superlattices.[1–13] These studies show the importance of the coupling between the CuO_2 planes for superconductivity. Most work has been concerned with the transition into the superconducting state at zero magnetic field. In this paper, however, we focus on the influence of a reduced dimensionality on transport at high magnetic fields, i.e., the influence of the dimensionality of the vortices on the superconducting transition temperature.

A consensus seems to have been reached that a three-dimensional (3D) disordered superconductor in a high magnetic field exhibits a phase transition to a truly superconducting vortex-glass (VG) phase.[14] Experimental evidence for this phase transition has in particular been obtained from the critical behavior of the transport properties of $YBa_2Cu_3O_{7-\delta}$ films.[15–22] According to theoretical predictions and numerical simulations,[14,23–28] the critical dimension for the formation of a VG phase at a finite temperature is somewhere between 2 and 3. Consequently, one does not expect a VG transition at any finite temperature for a strictly two-dimensional (2D) system. In this report, we present experimental data that support this notion.

The effects of a reduced dimensionality on the VG transition appear in various experiments. For $Bi_2Sr_2CaCu_2O_{8+\delta}$, the extreme anisotropy leads to various 2D-3D crossovers and a rather complex phase diagram.[29–31] $YBa_2Cu_3O_{7-\delta}$ samples of different type (films, disordered crystals, bulk ceramics) exhibit a 3D VG transition.[15–22] Finite-size effects show up if one dimension is reduced such as for thin films[18] or thin lines.[19] The present paper reports on a study of the finite-size effects on the VG transition in thin $YBa_2Cu_3O_{7-\delta}$ films. We find that the critical scaling behavior of the nonlinear current-voltage (I-V) curves, which signals the phase transition, deteriorates for ultrathin films which approach the 2D limit. In the true 2D limit, encountered for the thinnest film (16 Å) in our experiments, the I-V curves exhibit a different form that indicates a zero-temperature critical temperature for a 2D VG.

Various models have been proposed for the detailed nature of the glassy state in disordered type-II superconductors. The determining parameter in these models is the spatial structure of the defects responsible for the pinning of vortices. Pinning by random point defects, or, more generally, uncorrelated defects, will lead to a VG phase. Pinning by linelike or planelike defects along the external magnetic field (correlated defects) will give rise to a Bose-glass phase.[32] The VG and the Bose glass have very similar properties. Both exhibit a second-order phase transition with similar critical scaling, albeit with different scaling exponents.[33] In a previous report,[34] we have shown that for $YBa_2Cu_3O_{7-\delta}$ thin films made by laser ablation the dominant source of pinning is uncorrelated disorder, giving rise to a VG phase. In the present paper, we extend our study of these laser-ablated films to the properties of very thin films. The results are consistent with a 2D-3D dimensionality crossover for the VG phase.

This article is organized in the following way. In Sec. II we describe the experimental details of our experiment. Section III summarizes the scaling theory for the phase transition from a vortex liquid to a 3D VG. Section IV contains the experimental results and their analysis. Data are presented for three different regimes: (i) thick films

0163-1829/95/52(6)/4536(9)/$06.00

(film thickness $t = 3000$ Å) which display purely 3D behavior; (ii) films of intermediate thickness ($32 \leq t \leq 400$ Å) which show a crossover from 3D to 2D behavior; and (iii) data for an ultrathin (16 Å) film which displays purely 2D behavior. Some conclusions are given in Sec. V.

II. EXPERIMENTAL DETAILS

A. Samples

Epitaxial $YBa_2Cu_3O_{7-\delta}$ films were grown by laser ablation onto $SrTiO_3$ substrates. The thickness t of these films ranged from 3000 down to 16 Å, viz. 3000, 400, 200, 100, 32, and 16 Å. The films of thickness 100 Å or less were sandwiched in between two nonsuperconducting $PrBa_2Cu_3O_{7-\delta}$ layers. The $PrBa_2Cu_3O_{7-\delta}$ bottom layer (thickness typically 100 Å) served to provide a well matched buffer for epitaxial growth of the $YBa_2Cu_3O_{7-\delta}$. The top $PrBa_2Cu_3O_{7-\delta}$ layer (thickness typically 30 Å) served to protect the $YBa_2Cu_3O_{7-\delta}$ from degradation by exposure to the atmosphere. Electrical contacts were made by first removing the top $PrBa_2Cu_3O_{7-\delta}$ layer as well as part of the $YBa_2Cu_3O_{7-\delta}$ by Ar-ion milling through a metal shadow mask, followed by *in situ* deposition of 500 Å of Au through the same mask. The films were patterned with a resistless lithography technique based on local ablation by a pulsed laser. Four-probe patterns with a central stripe of typically 30×150 μm^2 were defined. Care was taken to minimize the laser power to prevent thermal damage of the film. For the films thicker than 100 Å the contacts were additionally annealed at 400 °C in flowing oxygen to further improve the contact resistance. The resulting contact resistance typically was substantially less than 1 Ω.

Figure 1 displays the resistivity versus the temperature for a selection of films at zero magnetic field and at a field of 5 T. As in all the experiments reported here, the magnetic field was oriented parallel to the film c axis. Figure 2 shows the superconducting transition temperature as a function of the film thickness for fields of 0, 2, and 5 T.

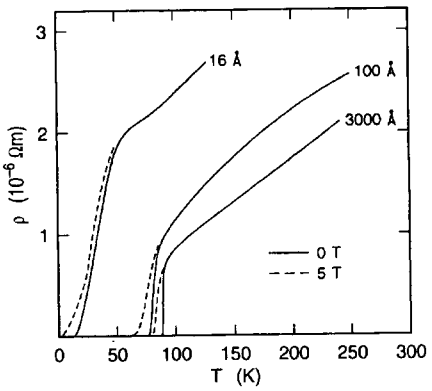

FIG. 1. Temperature dependence of the resistivity for three $YBa_2Cu_3O_{7-\delta}$ films of various thickness in magnetic fields of 0 and 5 T.

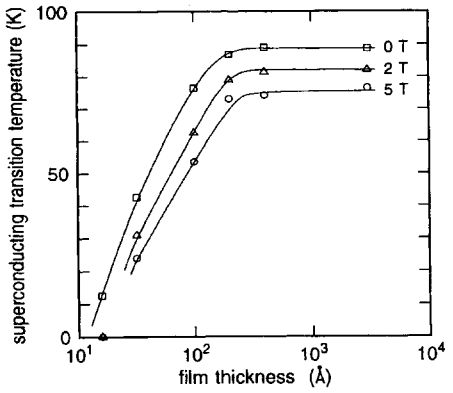

FIG. 2. Superconducting transition temperature versus the film thickness. At 0 T, T_c is defined as the temperature where the resistivity vanishes. At 2 and 5 T, the transition temperature is T_g as derived from the 3D critical-scaling analysis (cf. Sec. IV A). The solid lines are guides to the eye.

For the films thicker than 200 Å, T_c approaches a thickness-independent value of 89 K at zero field. For films with thickness below 200 Å, T_c can be seen to drop rapidly from 89 to 13 K for the 16 Å film. This drop in T_c is in agreement with previous reports.[5,8] A similar effect is observed in the superconducting transition temperature at high magnetic fields (the VG critical temperature; see Sec IV A). Again, a strong decrease is observed below about 200 Å. For the thinnest film, the VG transition temperature at high field has completely vanished.

B. Experimental setup

Figure 3 shows the experimental setup used for measuring the nonlinear I-V characteristics described in

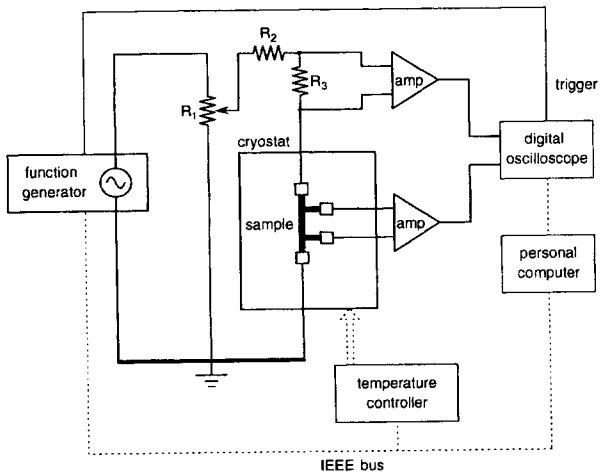

FIG. 3. Schematic diagram of the setup used for the nonlinear I-V measurements.

this article. An HP3325B function generator and a resistance network produce a sine-wave current with a frequency of approximately 10 Hz. This current is passed through the sample and a resistor R_3, which serves as a monitor for the current. The voltage over the sample and that over R_3 are each amplified by a battery-powered Stanford SRS560 low-noise preamplifier. Upon a trigger signal from the function generator, the amplified voltages are sampled for a duration of at least one period by the 8-bit analog-to-digital converters of a Tektronix TDS460 digital oscilloscope, and displayed as time traces. To eliminate noise and interference, these current and voltage traces are averaged over typically 5000 periods. This has the additional advantage of increasing the effective dynamic range of the digital scope to about 11 bit, i.e., to about three decades. After each measurement, the averaged voltage and current time traces are read out to a personal computer. In view of the limited dynamic range, each I-V curve is typically measured for three different amplitudes of the ac current. These amplitudes are chosen such that the resulting voltages span a total voltage range of about five to six decades. The function generator, the digital oscilloscope, and the temperature controller are controlled by the personal computer via the IEEE-488 bus. The data acquisition has been completely automated, enabling us to measure I-V curves for many temperatures. The time needed for collecting a typical set of 100–200 IV curves amounts to about three days.

Some advantages of the above ac measuring method are (i) the zero of the current and voltage signal can be determined with great precision, simply by taking the average of the current and the voltage over one period; (ii) voltages as small as a few nanovolts can be measured; and, most importantly, (iii) the shape of the measured I-V curves is reliable because the temperature does not vary appreciably over the course of a period of the current. The ac method ensures that any current-induced heating is averaged out to a steady temperature offset applying to the whole curve. Note here that the design of our cryogenic system is such that the relevant time constants ($\approx 10-10^2$ s) are long compared to the period of the ac current (≈ 0.1 s). In the use of a dc current for measuring I-V curves, by contrast, the temperature may rise substantially at the higher currents, which distorts the shape of the I-V curve.

III. THEORY OF 3D VORTEX-GLASS SCALING

Some of the VG scaling theory is briefly recapitulated in this section in order to provide the necessary background for the critical scaling analyses of the nonlinear I-V characteristics. For disordered 3D type-II superconductors a VG transition from a resistive vortex-liquid phase to a superconducting VG phase has been predicted.[14] As this VG transition is a second-order (continuous) transition, critical-scaling behavior is expected to occur near the transition. This implies that the I-V characteristics can be described in the form of a general scaling equation $V/I = \mathcal{R}_{\pm}(I,T)$, where $\mathcal{R}_{\pm}(I,T)$ is a scaling function for the resistance above (+) and below (−) the transition. The form of $\mathcal{R}_{\pm}(I,T)$ will be discussed below.

The relevant characteristic length scale, the VG correlation length ξ, is expected to diverge critically with the temperature at the VG phase transition temperature T_g according to a power law. That is,

$$\xi \propto 1/|T-T_g|^{\nu} , \tag{1}$$

with ν the static critical exponent. Further, a critical slowing down is expected for the dynamics near a continuous phase transition. This means, that a fluctuation of size ξ relaxes in a time τ, which critically diverges according to

$$\tau \propto \xi^z \propto 1/|T-T_g|^{z\nu} , \tag{2}$$

with z the dynamic critical exponent. The critical exponents z and ν are predicted to have universal values for all realizations of the VG, irrespective of the microscopic details of the disordered type-II superconductor.

A scaling relation can be constructed for the resistivity as a function of the applied current density. Above T_g, the linear resistance $R_{\rm lin}$ of a 3D correlation volume ξ^3 scales as the inverse of the lifetime of fluctuations in this volume, i.e., $R_{\rm lin} \propto 1/\xi^z$. The linear resistivity $\rho_{\rm lin}$ thus scales as $R_{\rm lin}\xi^2/\xi \propto \xi^{1-z}$. Above T_g, the current density J_{nl} where the current density-electric field (E-J) curves cross over from an Ohmic current dependence at low current densities to a nonlinear dependence at high current densities on ξ as $J_{nl} \propto T/\xi^2$.[14] The picture behind this scaling relation is that the applied current density J induces vortex excitations with a characteristic length scale L that is given by

$$L = (k_B T/\Phi_0 J)^{1/2} , \tag{3}$$

with $\Phi_0 = h/2e$ the magnetic flux quantum. In other words, with a certain J one probes the vortices at a certain length scale L. Above T_g, the response to a current density is linear for small J such that $L > \xi$. For this case, one probes a volume L^3 that contains many correlation volumes ξ^3, and accordingly vortices act independently, i.e., they behave like a liquid. The response becomes nonlinear for large J such that $L < \xi$. Here, one probes the glassy vortex dynamics *within* a correlation volume. As T_g is approached, ξ grows to infinity, and J_{nl} vanishes.

These scaling relations are used to construct a general scaling function. Near the phase transition the resistivity $\rho(J) \equiv E(J)/J$, in which E is the electric field and J is the current density, should exhibit a scaling dependence on J according to

$$\frac{\rho(J)}{\rho_{\rm lin}} = \mathcal{J}_{\pm}\left[\frac{J}{J_{nl}}\right] , \tag{4}$$

where $\mathcal{J}_{\pm}$ is a scaling function. With Eq. (1) inserted, Eq. (4) becomes

$$\frac{E}{J|T-T_g|^{\nu(z-1)}} = \mathcal{J}_{\pm}\left[\frac{J}{T|T-T_g|^{2\nu}}\right] . \tag{5}$$

The exact functional dependence of $\mathcal{F}_{\pm}$ is unknown, but we do know its limiting behavior. Above T_g and for $J < J_{nl}$, $\mathcal{F}_+ \rightarrow 1$, so that the resistivity equals the linear resistivity. At T_g, the VG correlation length ξ grows to infinity. As E and J must have finite values, the scaling function $\mathcal{F}_{\pm}(x)$ should be proportional to $x^{(z-1)/2}$. At T_g, E thus depends on J according to a power law

$$E \propto J^{(z+1)/2} . \tag{6}$$

Below T_g, the E-J curves approach an exponential dependence according to

$$E/J \propto \exp[-(J_0/J)^{\mu}] , \tag{7}$$

or, $\mathcal{F}_- \rightarrow \exp(-1/x^{\mu})$, with J_0 a constant and μ a glass exponent, $0 < \mu \leq 1$. Equation (7) implies that the resistivity of the VG phase vanishes in the limit of a vanishing applied current density, i.e., the VG phase is truly superconducting.

IV. EXPERIMENTAL RESULTS AND ANALYSES

A. Thick films ($t = 3000$ Å)

In this section we show an example of the 3D VG critical-scaling behavior encountered for thick $YBa_2Cu_3O_{7-\delta}$ films where no finite size effects are observed. We present results for a 3000 Å thick film. In zero magnetic field the film had a superconducting transition temperature $T_c = 88.7$ K. Nonlinear I-V curves were taken at temperatures around the VG transition in a magnetic field at 2 T directed along the film c axis. From a critical-scaling analysis of these curves, we can extract the optimum values for T_g, z, and ν. Below, we give a detailed demonstration of the scaling procedure.

Figure 4 shows a selected set of the E-J curves in a log-log plot. These E-J curves display the "standard" critical VG behavior. Above T_g, the E-J curves cross over from Ohmic behavior at low currents to a power-law dependence at high currents. The E-J curve taken at T_g displays a power-law dependence according to Eq. (6) over its whole current range. Below T_g, the E-J curves at low currents display an exponential dependence according to Eq. (7), whereas at higher currents they cross over to a power-law dependence. The E-J curves—when plotted double logarithmically—thus cross over from a positive curvature above T_g to a negative curvature below T_g. In order to determine T_g, therefore, we fit the E-J curves to a second-order polynomial of the form $\log_{10}E = a_0 + a_1 \log_{10}J + a_2 \log_{10}{}^2J$. The coefficient a_2 of this phenomenological fit is subsequently used as a measure of the curvature of each E-J curve. In Fig. 5, a_2 is plotted versus the temperature T. From the zero point of a_2 the transition temperature T_g is determined. We thus find that the VG transition occurs at $T_g = 82.2 \pm 0.1$ K.

According to Eq. (5) we expect the E-J isotherms to collapse onto a single scaling curve if we plot each isotherm as $E/J|T-T_g|^{\nu(z-1)}$ versus $J/T|T-T_g|^{2\nu}$, if at least the proper values for T_g, z, and ν are inserted. The individual scaled E-J isotherms then combine to a single curve, which is the visualization of the scaling function $\mathcal{F}_{\pm}$. To illustrate the buildup of the scaling collapse, Fig. 6 shows a scaling "collapse" which is constructed from a very small subset (8 out of about 100) of the E-J isotherms. The scaling curve consists of two distinct branches: the upper branch consists of the E-J curves taken above T_g and visualizes $\mathcal{F}_+$. The lower branch consists of the E-J curves taken below T_g and visualizes $\mathcal{F}_-$. The data in the linear regime contribute to the flat horizontal tail of the upper branch (cf. the curve taken at 86.00 K). The data taken near T_g collapse near the meeting point of the upper and lower branches (curves at 82.31 and 82.11 K), and the data taken at the lowest temperatures collapse in the tail of the lower branch.

For the proper values of T_g, z, and ν all data will collapse onto a scaling curve. To determine these values, scaling plots for various T_g, z, and ν are compared with

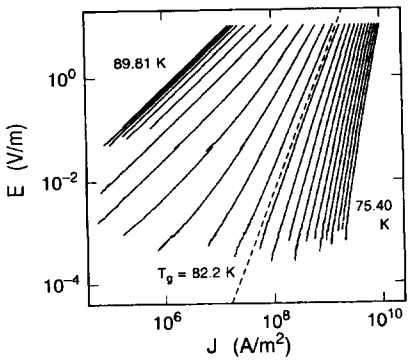

FIG. 4. Log-log plot of a selection of E-J isotherms, taken at temperatures near the VG transition in the 3000 Å $YBa_2Cu_3O_{7-\delta}$ film at $H = 2$ T. Consecutive E-J isotherms differ by about 0.60 K. The dashed line indicates the power-law dependence at the VG transition temperature T_g.

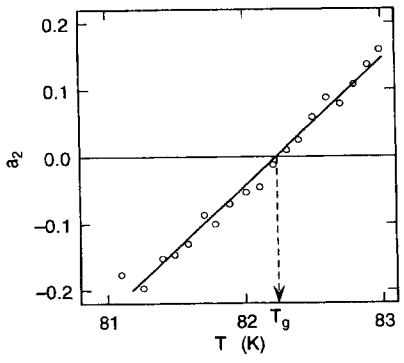

FIG. 5. Coefficient a_2 versus the temperature T as derived from fits of E-J such as in Fig. 4 to the polynomial $\log_{10}E = a_0 + a_1 \log_{10}J + a_2 \log_{10}{}^2J$. The solid line is a linear fit to the output values for a_2. The dashed arrow denotes T_g as derived via $a_2 = 0$.

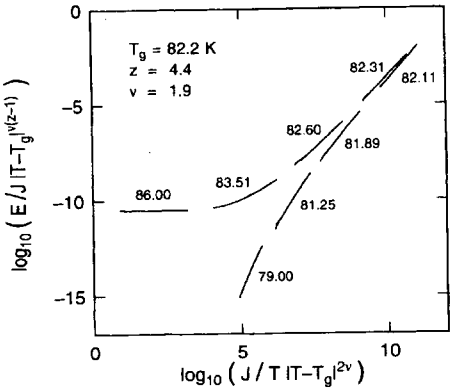

FIG. 6. Scaling collapse of a small selection of *E-J* isotherms taken near the VG transition in the 3000 Å $YBa_2Cu_3O_{7-\delta}$ film at $H=2$ T. Labels indicate the temperatures at which the *E-J* curves were taken. The values used for T_g, z, and ν are the values for optimum scaling collapse.

regard to the extent that the *E-J* data collapse onto a single sharp curve. In other words, deviations from a single well defined curve are minimized. Figure 7 shows the effect of variation of ν on the scaling collapse. A choice of ν deviating from the optimum value mainly affects the collapse in the tails of the scaling curve. The collapse worsens in the sense that both tails grow "thicker" as ν is chosen further away from its optimum value. Figure 8 similarly shows the sensitivity of the collapse to the dynamic exponent z. A nonoptimal choice of z additionally strongly affects the scaling collapse near T_g: successive *E-J* curves no longer align onto a single scaling curve, but instead are stacked like roof tiles. Variation of T_g has a very similar effect. Determination of the optimum combination of z and T_g is complicated by the strong correlation between these two parameters. This can be seen in Fig. 9, which shows a very elongated error ellipse. For this reason, we adopt T_g as obtained from the procedure leading to Fig. 5. This value approximately coincides with the center of the error ellipse, as is to be expected.

For the case in point of the 3000 Å $YBa_2Cu_3O_{7-\delta}$ film at 2 T, we thus find that the nonlinear *E-J* curves obey the three-dimensional scaling with an optimum scaling occurring for the combination $T_g=82.2\pm0.1$ K, $z=4.4\pm0.1$, and $\nu=1.9\pm0.2$. Similar exponents were found for other magnetic fields and the other 3000 Å films.

B. Thin films ($32 \leq t \leq 400$ Å)

Figure 10 shows a selected set of *E-J* curves for a 100 Å film at 5 T. Results for other fields and for films with

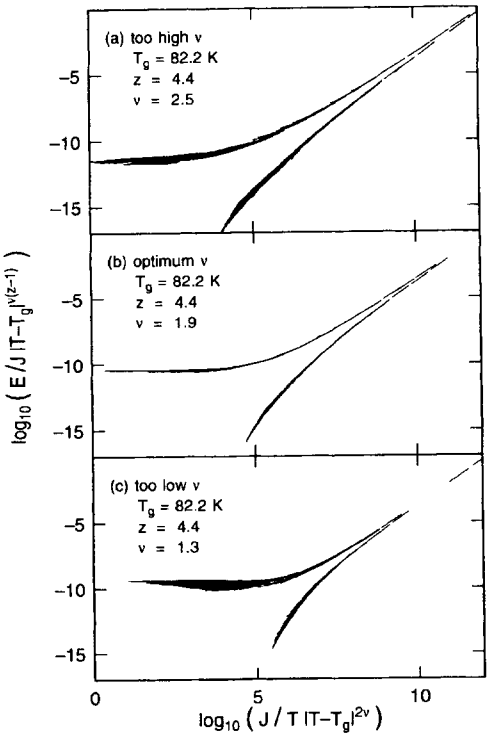

FIG. 7. Scaling collapse of more than 100 *E-J* curves for three different values of ν. Frames (a), (b), and (c) refer to values for ν above, at, and below the optimum, respectively. The data are taken in the 3000 Å $YBa_2Cu_3O_{7-\delta}$ film at $H=2$ T.

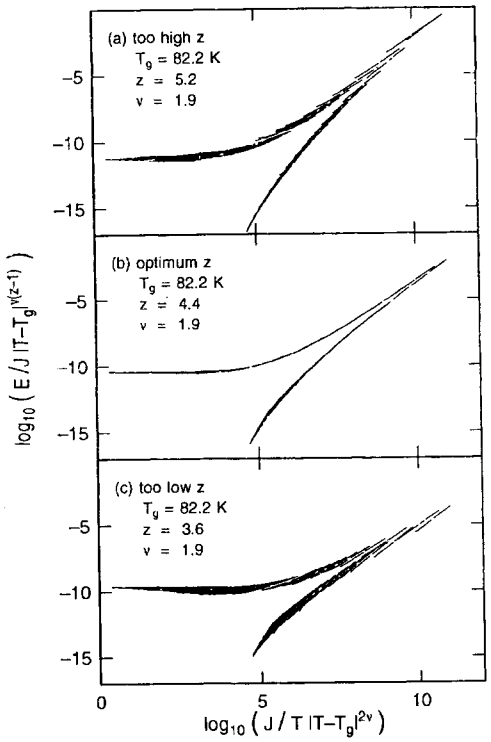

FIG. 8. Scaling collapse of more than 100 *E-J* curves for three different values of z. Frames (a), (b), and (c) refer to values for z above, at, and below the optimum, respectively. The data are taken in the 3000 Å $YBa_2Cu_3O_{7-\delta}$ film at $H=2$ T.

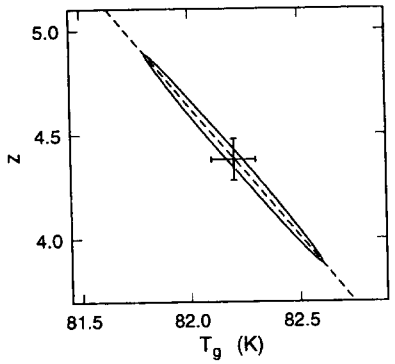

FIG. 9. Error ellipse of z versus T_g, based on the quality of the scaling plots. The error bar of T_g is derived from the procedure leading to Fig.5. The error bar in z then follows from its correlation with T_g.

thicknesses between 400 and 32 Å are very similar. In order to appreciate the deviations of these data from purely 3D behavior, one should compare Fig. 10 to the results obtained in the thick ($t=3000$ Å) film of the previous subsection (Fig. 4). The difference is most apparent at the VG transition temperature T_g. For the thick film data, Fig. 4, one can straightforwardly point out the temperature T_g at which the corresponding E-J curve obeys a pure power law according to Eq. (6). At T_g, the E-J curves can clearly be seen to crossover from a positive curvature at $T>T_g$ to a negative curvature at $T<T_g$.

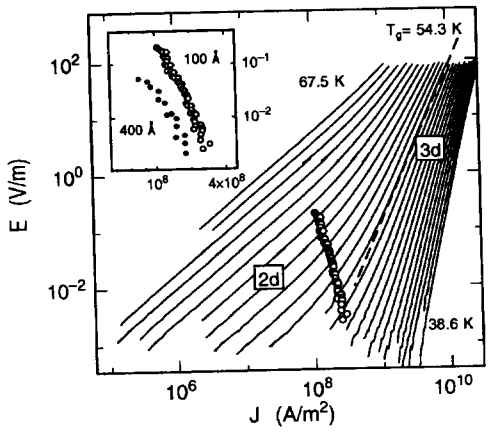

FIG. 10. Selected E-J isotherms for the 100 Å film at 5 T. Consecutive E-J curves differ by approximately 1.2 K. The thick solid line denotes the E-J curve at T_g. The open dots represent the crossover points where deviations from 3D scaling set in, as derived from Fig. 11. The data in the upper right corner (labeled 3D) show scaling behavior according to the VG theory, whereas the data at lower left (labeled 2D) deviate from 3D scaling. The inset shows the 2D-3D crossover points found for the 100 Å and the 400 Å film at a magnetic field of 5 T.

For the thin film data of Fig. 10, however, it is impossible to point out a temperature at which the corresponding E-J curve over its whole J-range obeys a pure power law: the low-current Ohmic dependence of the E-J curves persists down to temperatures at which the high-current part manifestly displays the negative curvature associated with the VG phase.

To further investigate the differences from the 3D case, we now turn to a critical-scaling analysis. In Fig. 11, it is attempted to apply 3D critical scaling to the data of Fig. 10 for the 100 Å film. It appears impossible to adjust the scaling parameters T_g, z, and ν in such a way as to arrive at a collapse onto a single well-defined curve for the whole E-J curves. This show that simple 3D scaling does not apply for a film of this thickness. However, it *is* possible to obtain a good collapse if we restrict the data to the high-current parts. This is shown in the inset of Fig. 11. For this plot, only those parts of the same E-J curves with $J>2\times10^8$ A/m^2 have been scaled by use of the method described in Sec. IV A. Apparently, the 3D VG behavior is recovered at high current densities. Figure 11 shows the scaling collapse of the full E-J curves, where the scaling parameters T_g, z, and ν, however, were optimized for the high-current parts of these curves. The low-current parts then bend away from the scaling curve, appearing as horizontal lines in Fig. 11. This is consistent with a linear resistivity at low J. For each isotherm, we may now define a 2D-3D crossover point as the intersection of the low-current asymptotic value of $E/J|T-T_g|^{\nu(z-1)}$ and the scaling curve (cf. dashed lines in Fig. 11). The result, the open circles in Fig. 10, visualizes the crossover from Ohmic resistivity in the 2D regime to scaling behavior in the 3D regime. Quite interestingly, the crossover takes place at a current density of $\sim2\times10^8$ A/m^2, which is consistent with the following

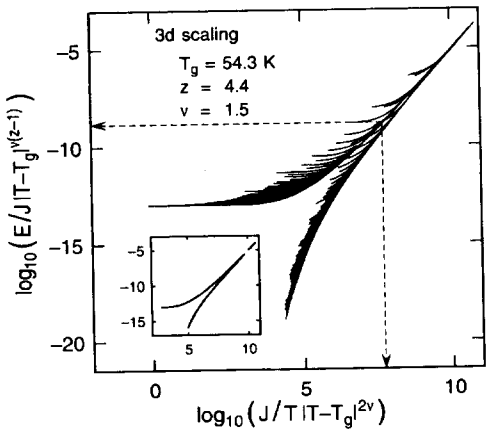

FIG. 11. The 3D scaling collapse of the E-J data of Fig. 10 for the 100 Å film. The dashed lines illustrate the definition of points that characterize the crossover from 3D scaling to 2D deviations (open dots in Fig. 10). The inset shows the scaling collapse of only the high-current parts of the E-J curves, using the T_g, z, and ν values indicated in the main plot.

picture. With an applied current density J, one creates vortex excitations with a typical length scale along the film c axis[14]

$$L_c = \sqrt{\gamma} L \sim (\gamma k_B T/\Phi_0 J)^{1/2} , \tag{8}$$

where γ is the anisotropy parameter, which for $YBa_2Cu_3O_{7-\delta}$ amounts to 0.2 According to Eq. (8) the 2D-3D crossover current density is equivalent with a probing length of ~ 200 Å, which indeed is of the same order of magnitude as the film thickness of 100 Å. Note that Eq. (8) is a rough scaling estimate only. For current densities larger than this 2D-3D crossover current density, the vortices are probed on length scales smaller than the film thickness, and exhibit 3D behavior. For current densities smaller than the 2D-3D-crossover current density, the vortices are probed on length scales larger than the film thickness. For this case, the E-J curves display 2D behavior. When scaled according to the 3D scaling relation, they deviate from the main (3D) scaling collapse. Comparing the results for the 400 Å film and the 100 Å film in the inset of Fig. 10, we see that the crossover between 2D and 3D behavior shifts to lower current densities in thicker films, as expected from this argument. For even thicker films, the 2D-3D crossover line moves out of the measurement range.

An alternative way to illustrate the finite-size effect is to directly estimate the VG correlation length along the c axis (ξ_c). This correlation length can be derived from the current density J_{nl} at which the E-J curves cross over from the Ohmic dependence at low J to a nonlinear current dependence at high J. At J_{nl}, the probing length L_c along the c axis roughly equals ξ_c, and with Eq. (8) we find $\xi_c = (\gamma k_B T/\Phi_0 J_{nl})^{1/2}$. For each isotherm, we extract J_{nl} from the point where the E-J curves start to deviate from the low-J linear behavior. Somewhat arbitrarily, we define J_{nl} as the value of J for which we have $\partial \ln E/\partial \ln J = 1.2$. The use of various other criteria for the onset of nonlinearity yields essentially the same results. Figure 12 shows the resulting c-axis correlation length as a function of the reduced temperature. Far from the transition, ξ_c follows the 3D critical divergence $\xi_c \propto 1/(T-T_g)^{\nu}$ [cf. Eq. (1)] with $\nu = 1.7$ (solid lines), but ξ_c appears to level off to a constant plateau (dashed lines) upon approach of T_g. The plateau value roughly scales with the film thickness (see inset). Typical numbers equal the film thickness to within a factor of up to 5, which is quite satisfactory in view of the crude assumptions made in Eq. (8) as well as in the definition of J_{nl}. These findings indicate that the growth of the 3D VG correlation length indeed is limited by the film thickness.

C. Ultrathin films ($t = 16$ Å)

As reported previously in Ref. 18, the behavior of vortices turns completely two-dimensional in our thinnest film of 16 Å. The 3D VG transition, as observed in the thicker films, is completely absent in this film. A scaling collapse of the E-J curves according to the 3D scaling equation (5) cannot be achieved for any combination of T_g, z, and ν. Three-dimensional VG order thus appears to be absent. However, 2D VG correlations may develop towards 0 K, the critical temperature for a 2D VG as expected from the theory.[14,23–28] The relevant length scale of these correlations, the 2D VG correlation length ξ_{2D}, is expected to diverge critically at zero temperature according to

$$\xi_{2D} \propto 1/T^{\nu_{2D}} . \tag{9}$$

An applied current density J creates 2D vortex excitations with a characteristic length $L = k_B T/\Phi_0 J$. Analogous to the 3D case, the response to a current density is linear at small current densities when $L > \xi_{2D}$, and becomes nonlinear at higher current densities when $L < \xi_{2D}$. Thus the current density at which nonlinearity sets in is given by $J_{nl} = k_B T/\Phi_0 \xi_{2D}$. We have deduced J_{nl} from the nonlinear E-J curves for the 16 Å film (cf. Ref. 18). The temperature dependence of the 2D VG correlation length ξ_{2D} as derived from J_{nl} is shown in Fig. 13. From this figure we indeed see that ξ_{2D} diverges with decreasing temperature, reaching values of up to 0.3 μm near 5 K. Equation (9) yields a good fit to the data (solid lines in Fig. 13). This constitutes experimental evidence for a zero critical temperature for a 2D VG. From the fits, we find $\nu_{2D} = 2.0 \pm 0.3$, which agrees very well with theoretical estimates of ν_{2D} that range from 1.8 to 2.3.[14,23–28]

For a 2D VG, Fisher, Tokuyasu, and Young[23] have predicted a temperature dependence of the linear resistivity R_{lin} according to

$$R_{lin} \propto \exp[-(T_0/T)^p] , \tag{10}$$

with $p = 1$ for the case of classical thermal activation of vortices over barriers, whereas $p \approx 0.7$ if vortex motion proceeds through quantum tunneling. In order to test

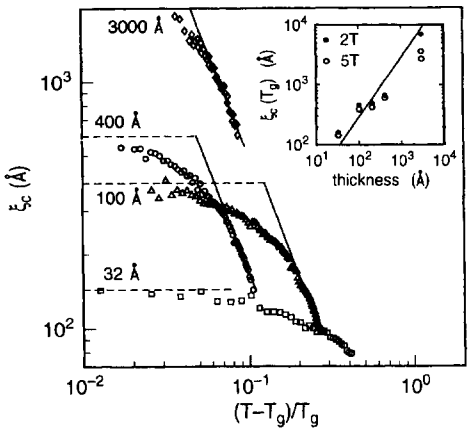

FIG. 12. The correlation length along the film c axis ξ_c at 5 T versus the reduced temperature for films of various thickness. The solid lines denote the critical behavior $\xi_c \propto 1/(T-T_g)^{1.7}$. The dashed lines indicate the leveling off upon approach of T_g. The inset shows the plateau ξ_c versus the nominal film thickness. The solid line denotes a linear relationship.

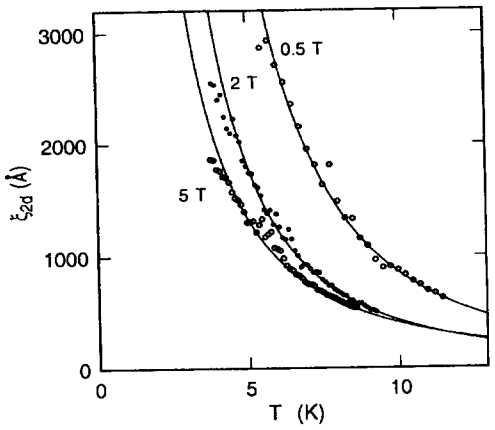

FIG. 13. The 2D VG correlation length ξ_{2D} as a function of temperature of the 16 Å film at various magnetic fields. The solid lines are fits of the data to a $\xi_{2D} \propto 1/T^{\nu_{2D}}$ dependence. At 0.5, 2, and 5 T, we find $\nu_{2D}=2.3$, 2.1, and 1.7, respectively.

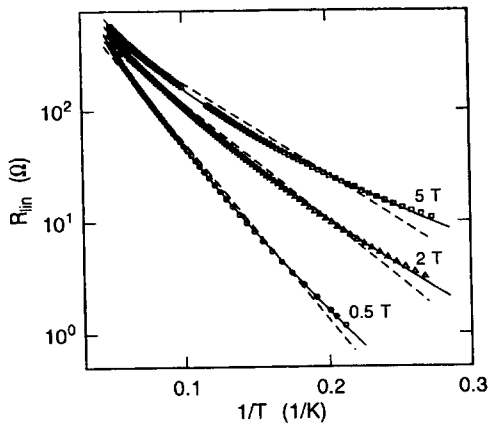

FIG. 14. Linear resistance versus inverse temperature $1/T$ for the 16 Å film at 0.5, 2, and 5 T in a semilog plot. The dashed lines are fits to thermally activated vortex motion, i.e., Eq. (10) with $p=1$. The solid lines are fits to the same equation with p as a free parameter. At 0.5, 2, and 5 T we find $p=0.65$, 0.58, and 0.41, respectively.

this, we have plotted the linear resistivity in an Arrhenius plot; see Fig. 14. From fits Eq. (10) we find $p=0.55\pm0.12$. This is clearly less than 1. In other words, the data do not show a simple thermally activated temperature dependence (cf. the dashed lines in Fig. 14). The low experimental value for p may be taken as an indication that the vortex motion proceeds through quantum tunneling.

V. CONCLUSIONS

The nonlinear transport characteristics of very thin $YBa_2Cu_3O_{7-\delta}$ films in a high magnetic field appear to be different from those in 3D systems. The difference may be understood in terms of a finite-size effect, in the sense that a crossover from 3D to 2D behavior occurs when the vortices are probed on length scales exceeding the film thickness. The picture arises from a critical scaling analysis of the data. It is further supported by the temperature dependence of the 3D VG correlation length, which levels off at the film thickness upon approach of T_g. The results indicate that a VG phase transition does occur at finite temperature in 3D systems, but not in 2D systems. In the latter an onset of 2D VG correlations occurs towards zero temperature. This is demonstrated in our thinnest film, which displays a critically diverging 2D VG correlation length in the limit of zero temperature.

ACKNOWLEDGMENTS

We would like to thank H. W. de Wijn for useful discussions. The work was in part supported by the U.S. Office of Naval Research as well as by the Netherlands Foundation "Fundamenteel Onderzoek der Materie" (FOM) and the "Nederlandse Organisatie voor Wetenschappelijk Onderzoek" (NWO).

*Present address: IBM T. J. Watson Research Center, P.O. Box 218, Yorktown Heights, NY 10598.
†Present address: Department of Applied Physics, Delft University of Technology, Lorentzweg 1, 2628 CJ Delft, The Netherlands.

[1]J. M. Triscone, M. G. Karkut, L. Antognazza, O. Brunner, and Ø. Fischer, Phys. Rev. Lett. **63**, 1016 (1989).
[2]Q. Li, X. X. Xi, X. D. Wu, A. Inam, S. Vadlamannati, W. L. McLean, T. Venkatesan, R. Ramesh, D. M. Hwang, J. A. Martiez, and L. Nazar, Phys. Rev. Lett. **64**, 3086 (1990).
[3]D. H. Lowndes, D. P. Norton, and J. D. Budai, Phys. Rev. Lett. **65**, 1160 (1990).
[4]G. Jakob, I. Hahn, C. Stölzel, C. Tomé-Rosa, and H. Adrian, Europhys. Lett. **19**, 135 (1992).
[5]T. Terashima, K. Shimura, Y. Bando, Y. Matsuda, A. Fujiyama, and S. Komiyama, Phys. Rev. Lett. **67**, 1362 (1991).
[6]Vadlamannati, Q. Li, T. Venkatesan, W. L. McLean, and P. Lindenfeld, Phys. Rev. B **44**, 7094 (1991).
[7]Y. Matsuda, S. Komiyama, T. Onagi, T. Terashima, K. Shimwa, and Y. Bando, Phys. Rev. B **48**, 10 498 (1993).
[8]C. Kwon, Q. Li, X. X. Xi, S. Battacharaya, C. Doughty, T. Venkatesan, H. Zhang, J. W. Lynn, J. L. Peng, Z. Y. Li, N. D. Spencer, and K. Feldman, Appl. Phys. Lett. **62**, 1289 (1993).
[9]T. Schneider, Z. Phys. B **85**, 187 (1991).
[10]K. Michielsen, T. Schneider, and H. De Raedt, Z. Phys. B **85**, 15 (1991).
[11]T. Schneider and J. P. Loquet, Physica C **179**, 125 (1991).

[12]T. Schneider, Z. Gedik, and S. Ciraci, Z. Phys. B **83**, 313 (1991).
[13]M. Rasolt, T. Edis, and Z. Tesanovic, Phys. Rev. Lett. **66**, 2927 (1991).
[14]M. P. A. Fisher, Phys. Rev. Lett. **62**, 1415 (1989); D. S. Fisher, M. P. A. Fisher, and D. A. Huse, Phys. Rev. B **43**, 130 (1991).
[15]R. H. Koch, V. Foglietti, W. J. Gallagher, A. Gupta, and M. P. A. Fisher, Phys. Rev. Lett. **63**, 1511 (1989); R. H. Koch, V. Foglietti, and M. P. A. Fisher, *ibid.* **64**, 2586 (1990).
[16]H. K. Olsson, R. H. Koch, W. Eidelloth, and R. P. Robertazzi, Phys. Rev. Lett. **66**, 2661 (1991).
[17]C. Dekker, W. Eidelloth, and R. H. Koch, Phys. Rev. Lett. **68**, 3347 (1992).
[18]C. Dekker, P. J. M. Wöltgens, R. H. Koch, B. W. Hussey, and A. Gupta, Phys. Rev. Lett. **69**, 2717 (1992).
[19]J. Ando, H. Kubota, and S. Tanaka, Phys. Rev. Lett. **69**, 2851 (1992).
[20]D. G. Xenikos, J. T. Kim, and T. R. Lemberger, Phys. Rev. B **48**, 7742 (1993).
[21]J. Kötzler, M. Kaufmann, G. Nagielski, R. Behr, and W. Assmus, Phys. Rev. Lett. **72**, 2081 (1994).
[22]J. Kötzler, G. Nagielski, M. Baumann, R. Behr, F. Goerke, and E. H. Brandt, Phys. Rev. B **50**, 3384 (1994).
[23]M. P. A. Fisher, T. A. Tokuyasu, and A. P. Young, Phys. Rev. Lett. **66**, 2931 (1991).
[24]J. D. Reger, T. A. Tokuyasu, A. P. Young, and M. P. A Fisher, Phys. Rev. B **44**, 7147 (1991).
[25]M. J. P. Gingras, Phys. Rev. B **45**, 7547 (1992).
[26]J. D. Reger and A. P. Young, J. Phys. A **26**, L1017 (1993).
[27]R. A. Hyman, M. Wallin, M. P. A. Fisher, S. M. Girvin, and A. P. Young (unpublished).
[28]Note that the existence of a finite-temperature phase transition in the numerical simulations of a 3D VG appears to be model dependent; see H. S. Bokil and A. P. Young, Phys. Rev. Lett. **74**, 3021 (1995). Also, it is useful to point out that most numerical simulations have considered the gauge glass rather than the vortex glass, i.e., a model with random magnetic flux rather than one with a uniform magnetic field and random point disorder. Both models are expected to exhibit similar properties. More work is needed, however, to establish this convincingly.
[29]H. Safar, P. L. Gammel, D. J. Bishop, D. B. Mitzi, and A. Kapitulnik, Phys. Rev. Lett. **68**, 2672 (1992).
[30]R. Cubitt, E. M. Forgan, G. Yang, S. L. Lee, D. McK. Paul, H. A. Mook, M. Yethiraj, P. H. Kes, T. W. Li, A. A. Menovsky, Z. Tarnawski, and K. Mortensen, Nature **365**, 407 (1993).
[31]H. Yamasaki, K. Endo, S. Kosaka, M. Umeda, S. Yoshida, and K. Kajimura, Phys. Rev. B **50**, 12 959 (1994).
[32]D. R. Nelson and V. M. Vinokur, Phys. Rev. Lett. **68**, 2398 (1992).
[33]The Bose-glass model predicts a critical-scaling equation which is the same as the one predicted by the VG model, i.e., Eq. (5), with different critical exponents z' and ν', however. These Bose-glass critical exponents can be simply expressed in the VG critical exponents z and ν, viz $z'=\frac{1}{2}(3z+1)$ and $\nu'=\frac{2}{3}\nu$. Critical scaling of the nonlinear current-voltage characteristics in itself therefore cannot be used to distinguish between the two models. However, by investigating critical scaling at different angles between the magnetic field and the sample; it can be deduced which model is relevant; see Ref. 34.
[34]P. J. M. Wöltgens, C. Dekker, J. Swüste, and H. W. de Wijn, Phys. Rev. B **48**, 16 826 (1993).